physica status solidi b
www.pss-b.com

Extended Positron-Trapping Defects in the Eu^{3+}-Doped $BaGa_2O_4$ Ceramics Studied by Positron Annihilation Lifetime Method

Halyna Klym, Ivan Karbovnyk, Andriy Luchechko, Yuriy Kostiv, and Anatoli I. Popov*

The $BaGa_2O_4$ ceramics doped with Eu^{3+} ions (1, 3 and 4 mol%) are obtained by solid-phase sintering. The evolution of defect-related extended free volumes in the $BaGa_2O_4$ ceramics due to the increase of the content of Eu^{3+} ions has been studied using the positron annihilation lifetime (PAL) spectroscopy technique. It is established that the increase in the number of Eu^{3+} ions in the basic $BaGa_2O_4$ matrix leads to the agglomeration of free-volume defects with their subsequent fragmentation. The presence of Eu^{3+} ions results in the expansion of nanosized pores and an increase in their number with their future fragmentation.

1. Introduction

The $BaGa_2O_4$ ceramics are considered as a promising material for use as an insulator in optoelectronic devices,[1,2] as a secondary coating for plasma panels,[3–5] etc.[6] The doping of impurities in the form of rare-earth ions leads to the expansion of the functional properties of such ceramics.[7]

Recent studies of materials similar to $BaGa_2O_4$ ceramics in both undoped and doped forms are mainly focused on the study of their luminescent properties.[1,8–14] These ceramics are a double oxide belonging to the quadrilateral frame topologies that exist in multiple polymorphs, which is important for luminescence studies because it exhibits luminescence without the inclusion of rare-earth ions. However, the most interesting is rare-earth-doped $BaGa_2O_4$ ceramics. Most investigations of such material are limited to X-ray diffraction (XRD), optical studies, etc.[15–24] Nevertheless, doping of such ceramics not only leads to modification of their luminescent properties and changes in phase composition, but also causes structural transformation.[25–27] Such significant transformation of the inner structure in ceramics facilitates the formation of additional defect-related free volumes.[28–33]

Among the less conventional but promising methods to study the defect-related free volumes in solids of different structural types is positron annihilation lifetime (PAL) spectroscopy.[34,35] This technique has long been serving as a tool for structural analysis of such functional materials as ceramics,[36,37] glass,[38] polymers,[39] nanocomposites,[40] etc. Researchers in the field have presented a number of approaches to the analysis of PAL spectra of ceramic materials and to the proper decomposition of such spectra into different numbers of components.[41] We have also contributed to the topic using the PAL method to study changes in free volume in spinel ceramics,[42–44] chalcogenide glasses[45,46] under the influence of technological modification, etc. It was shown that functional ceramics are characterized by the decomposition of the PAL spectrum into two, three, and four components depending on the developed porous structure of materials.

It was concluded that for functional ceramic materials a pair of PAL channels is enabled: positron trapping (components with shorter and medium lifetimes) and o-Ps decaying (component with longer lifetime). Generally, these processes are independent ones. However, if trapping sites emerge in the vicinity of grain boundaries neighboring free-volume pores, they can become mutually interconnected thus bringing a significant complication to the measured PAL spectra. According to the two-state positron trapping model, in oxide ceramics, the first component reflects mainly microstructural specifics of spinel ceramics with characteristic octahedral and tetrahedral vacant cation sites along with a contribution from the annihilation of p-Ps atoms which is not considered in the further analysis.[42,47] Medium lifetime is related to the size of free-volume defects near grain boundaries and intensity reflects their amount. The third, longer component originates from the annihilation of o-Ps atoms in intrinsic nanopores of ceramics. However, the dedicated investigation of $BaGa_2O_4$ ceramics by the PAL method has not yet been conducted. Therefore, the goal of this work was to study the transformations of inner free volumes (extended defects at grain boundaries and nanopores) in $BaGa_2O_4$ ceramics doped with different amounts of Eu^{3+} ions using PAL method.

H. Klym, I. Karbovnyk, A. Luchechko, Y. Kostiv
Lviv Polytechnic National University
12 Bandera Str., 79013 Lviv, Ukraine
E-mail: halyna.i.klym@lpnu.ua

I. Karbovnyk, A. Luchechko
Ivan Franko National University of Lviv
50, Dragomanov Str., 79005 Lviv, Ukraine

A. I. Popov
Institute of Solid State Physics
University of Latvia
Kengaraga 8, LV-1063 Riga, Latvia

The ORCID identification number(s) for the author(s) of this article can be found under https://doi.org/10.1002/pssb.202100485.

DOI: 10.1002/pssb.202100485

2. Results and Discussion

The best fit parameters of PAL spectra for the studied ceramics calculated within the three-components procedure are listed in **Table 1** and graphically presented in **Figure 1**. It is established that with the rising of Eu^{3+} content in the $BaGa_2O_4$ matrix, an increase in the lifetime τ_1 and intensity I_1 of the first short-term component is observed. It is very likely that the structure of the principal ceramics phase is improved. However, when the Eu^{3+} ions concentration increases to 4 mol.%, the opposite trend starts to prevail. The lifetime τ_2 of the second component increases and intensity I_2 decreases with Eu^{3+} content (to 3 mol.%), while a further rise of Eu^{3+} ions (to 4 mol.%) leads to a decrease τ_2 and increase I_2.

As noted in ref. [42,43,47], the lifetime τ_2 of the second component should be associated with the capture of positrons by defect-related free volumes. According to XRD data,[48] undoped $BaGa_2O_4$ ceramics contain a large number of additional phases. As shown by the SEM method,[48] these phases are unevenly distributed in the volume of the ceramic and mainly localized near the grain boundaries. The extracted phases play the role of special centers of positron capture in the volume of ceramics.

Table 1. Lifetimes and intensities for undoped and Eu^{3+}-doped $BaGa_2O_3$ ceramics obtained at a three-components fitting procedure.

Sample	τ_1 [ns]	I_1 [%]	τ_2 [ns]	I_2 [%]	τ_3 [ns]	I_3 [%]
$BaGa_2O_4$	0.200 ± 0.002	83.3 ± 0.1	0.424 ± 0.001	14.9 ± 0.1	2.196 ± 0.001	1.8 ± 0.1
$BaGa_2O_4 + 1$ mol% Eu^{3+}	0.206 ± 0.002	85.0 ± 0.1	0.450 ± 0.001	13.2 ± 0.1	2.289 ± 0.001	1.8 ± 0.1
$BaGa_2O_4 + 3$ mol% Eu^{3+}	0.212 ± 0.002	89.9 ± 0.1	0.550 ± 0.001	7.9 ± 0.1	2.390 ± 0.001	2.2 ± 0.1
$BaGa_2O_4 + 4$ mol% Eu^{3+}	0.201 ± 0.002	83.3 ± 0.1	0.411 ± 0.001	14.4 ± 0.1	2.157 ± 0.001	2.4 ± 0.1

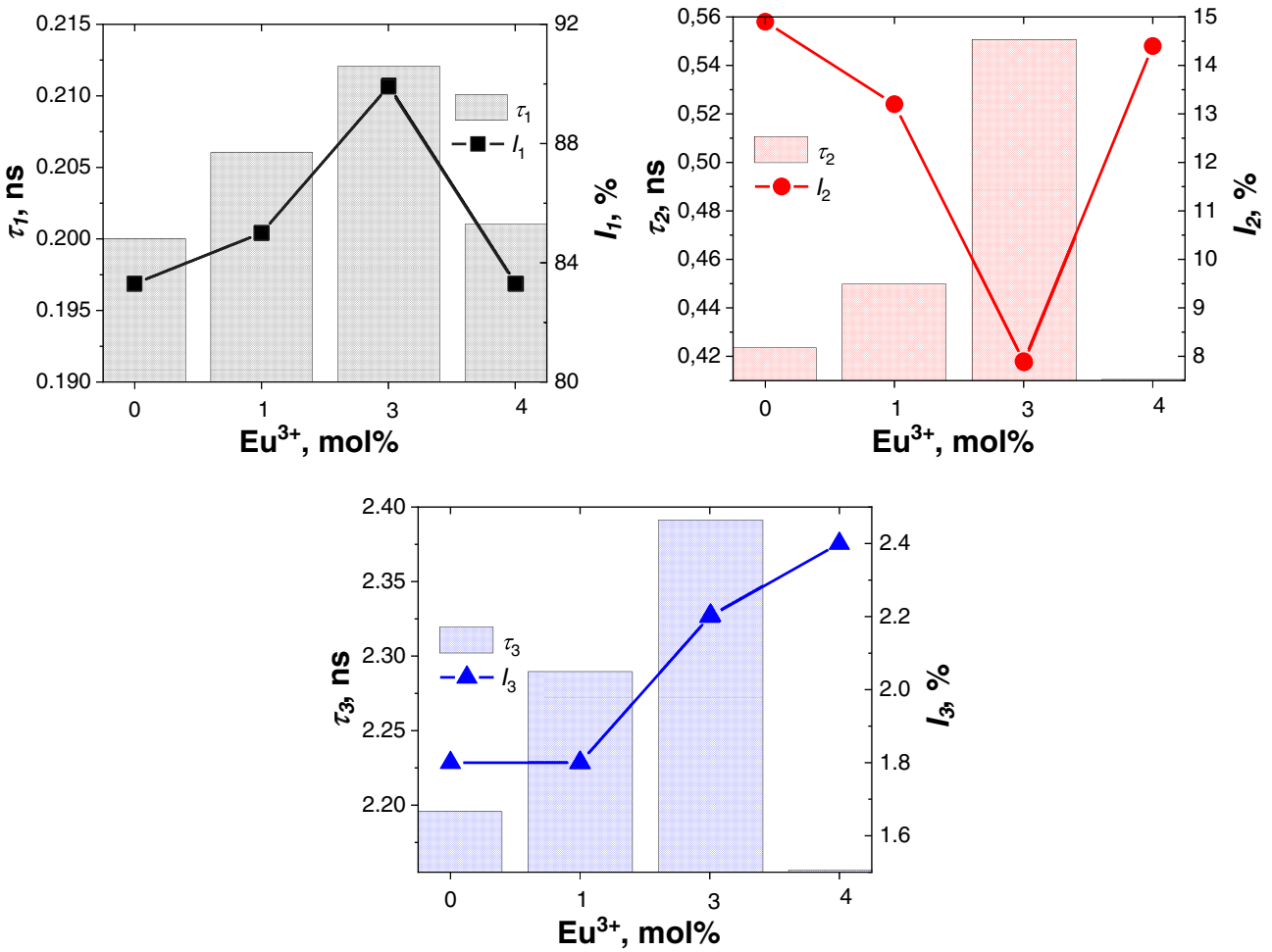

Figure 1. Dependences of lifetimes and intensities of positron annihilation lifetime (PAL) components on Eu^{3+} amount for undoped and Eu^{3+}-doped $BaGa_2O_4$ ceramics.

Table 2. Positron trapping parameters and nanopore radius for undoped and Eu^{3+}-doped $BaGa_2O_4$ ceramics.

Sample	$\tau_{av.}$ [ns]	τ_b [ns]	κ_d [ns^{-1}]	τ_{2-b} [ns]	τ_2/τ_b	R_3 [nm]
$BaGa_2O_4$	0.234	0.218	0.40	0.21	1.95	0.306
$BaGa_2O_4$ + 1 mol% Eu^{3+}	0.239	0.222	0.35	0.23	2.02	0.314
$BaGa_2O_4$ + 3 mol% Eu^{3+}	0.240	0.223	0.23	0.33	2.46	0.322
$BaGa_2O_4$ + 4 mol% Eu^{3+}	0.232	0.218	0.37	0.19	1.89	0.302

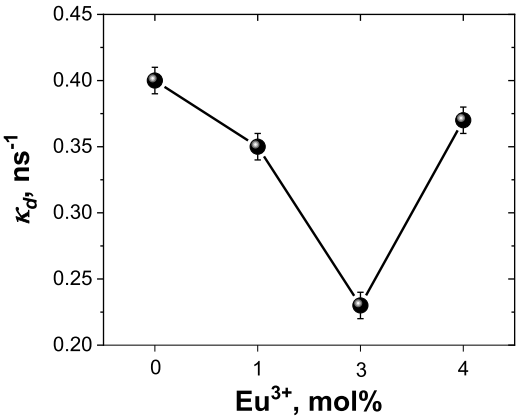

Figure 2. Dependences of positron trapping rate in defects κ_d on Eu^{3+} amount for undoped and Eu^{3+}-doped $BaGa_2O_4$ ceramics.

Since undoped $BaGa_2O_4$ ceramics contain two additional phases, positrons in such samples have statistically a better chance of being captured.

The lifetime τ_2 correlates with the size of free-volume defects, where positrons are captured and the intensity relates to their number. Thus, when the Eu^{3+} content increases to 3 mol%, agglomeration of free-volume defects occurs, while the supersaturation of the $BaGa_2O_4$ matrix with Eu^{3+} (up to 4 mol.%) leads to their fragmentation. The identified trends (**Table 2**) correlate with the positron trapping parameters $\tau_{av.}$, τ_b, κ_d calculated within the two-state positron trapping model.[47] The changes are best reflected in the positron trapping rate in defects κ_d (see

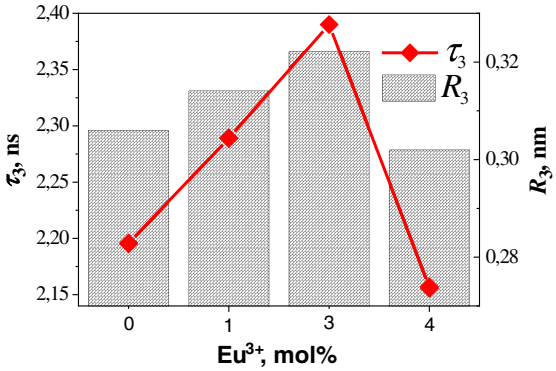

Figure 4. Dependencies of lifetime τ_3 and nanopores radius R_3 calculated according to the Tao–Eldrup model for undoped and Eu^{3+}-doped $BaGa_2O_4$ ceramics.

Figure 2). This value decreases with increasing Eu^{3+} content in ceramics and increases with its supersaturation of Eu^{3+} (up to 4 mol.%). The obtained values of τ_2/τ_b and $(\tau_2–\tau_b)$ parameters speak in favor of the similar nature of trapping sites. The characteristic size of these extended positron traps is close to that of single-double atomic vacancies.

Representatively, the evolution of defect-related free volumes near grain boundaries with increasing of Eu^{3+} ions in the $BaGa_2O_4$ ceramics is shown in **Figure 3**.

The third long-term component of the PAL spectrum (the second channel of positron annihilation with lifetime τ_3 and intensity I_3) is associated with the o-Ps decaying in nanopores.[42] As can be seen from Table 1, lifetime τ_3 and intensity I_3 increase with Eu^{3+} content in the $BaGa_2O_4$ ceramics (to 3 mol%). However, when the amount of Eu^{3+} ions further rises to 4 mol%, the lifetime τ_3 decreases and the intensity I_3 continues to go up. It is obvious that the presence of Eu^{3+} ions in the ceramic matrix leads to the expansion of nanosized pores and an increase in their number. However, supersaturation of ceramics with doped ions (to 4 mol.%) results in fragmentation of nanopores. The obtained trends are reflected in the radius of nanopores R_3 calculated by the Tao-Eldrup model (**Figure 4**).

Figure 5 explains this process in a schematic fashion, outlining the main stages of the evolution.

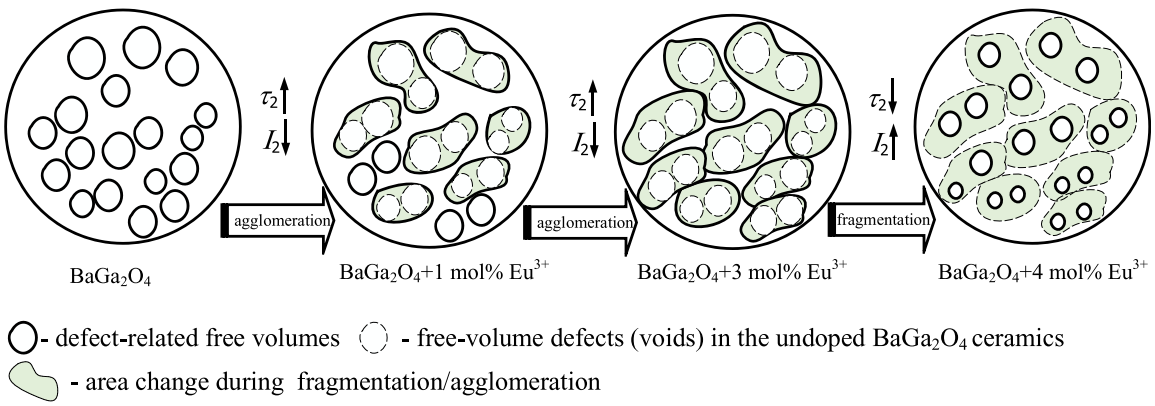

Figure 3. Diagram explaining the evolution of defect-related voids in $BaGa_2O_4$ ceramics caused by Eu^{3+} doping.

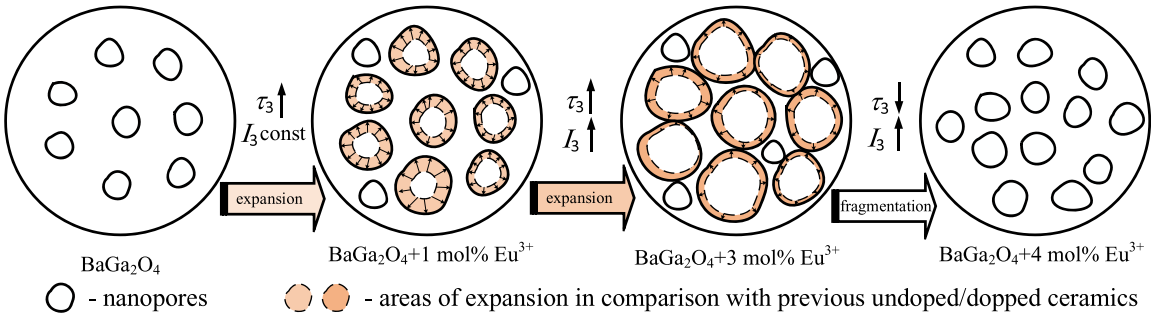

Figure 5. Diagram explaining the evolution of nanopores in $BaGa_2O_4$ ceramics caused by Eu^{3+} doping.

Summarizing, the PAL method can also be used to assess the size of nanopores in the undoped and doped ceramic materials.

3. Conclusion

The structural features and evolution of free-volume defects in the $BaGa_2O_4$ ceramics obtained by solid-phase synthesis from the initial $BaCO_3$ and Ga_2O_3 components with the addition of different amounts of Eu_2O_3 content (1, 3, and 4 mol%) were investigated.

Additional phases in ceramics are mainly localized near the grain boundaries and create defective centers for positron capture, as studied by PAL spectroscopy. Through the analysis of the second component of PAL spectra for the undoped and Eu^{3+}-doped $BaGa_2O_4$ ceramics, it was shown that the increase of Eu^{3+} content from 1 to 3 mol% leads to agglomeration of free-volume defects near grain boundaries of ceramics. At the same time, nanopores in ceramics expand, and their number increases. Further increase in the content of Eu^{3+} ions is accompanied with fragmentation of both free-volume defects and nanopores.

4. Experimental Section

Samples of the pure $BaGa_2O_4$ ceramics with Eu^{3+} impurities were prepared by high-temperature solid-phase synthesis similar to spinel-type $MgGa_2O_4$ ceramics.[49] Powders of $BaCO_3$ and Ga_2O_3 oxides with a purity of 99.99% were taken as starting components for synthesis. Isopropyl CH_3-CH(OH)-CH_3 alcohol was also used at the sintering of $BaGa_2O_4$-based ceramics.[48] The oxide mixtures were taken in a stoichiometric ratio of 1:1 mol. per 2 g of raw material. The content of Eu^{3+} ions (Eu_2O_3 with a purity of 99.99%) was determined to replace the equivalent molar content of Ga and Ba, respectively. The amount of Eu^{3+} ions was 0, 1, 3, and 4 mol%). The oxide mixture was thoroughly stirred in the agate solution for 6 h with the addition of isopropyl alcohol. The obtained raw material was dried in air for 1 h at a temperature of 80 °C. After that, the raw material was pressed under a pressure of 150 kg cm^{-2}, obtaining workpieces with a diameter of 6 mm and a thickness of 1.5 mm. The blanks were placed on a platinum substrate and annealed in a furnace at 1200 °C for 12 h in air. In the next stat, annealing was performed at 1300 °C for 5 h. The final ceramic samples were obtained in the form of tablets with a diameter of 4 mm and a thickness of 1 mm.[48]

The ORTEC system with ^{22}Na isotope as positron source was used for PAL measurements. Investigation was performed at 22 °C and relative humidity of 35% for two identical ceramic samples placed in a sandwich configuration as described in detail in ref. [42].

The measured PAL spectra were calculated using LT software[50] involving a three-component fitting procedure (lifetimes τ_1, τ_2, τ_3 and intensities I_1, I_2, I_3), which is considered a fair approach for spinel ceramics with branched porous structure.[47,51] The resulting inaccuracy in the positron lifetime of the first component τ_1 was $\pm$0.002 ns and errors for positron lifetimes of the second and third components (τ_2 and τ_3) were $\pm$0.001 ns. The error bar for intensities of all component is $\pm$0.1%.

Parameters such as the average lifetime of positrons τ_{av}, the lifetime of positrons in defect-free bulk τ_b and the rate of positron trapping in defects κ_d were obtained using a two-stage positron trapping model.[47] The τ_2–τ_b difference (which describes the size of the free-volume defects where positrons are trapped) and the τ_2/τ_b ratio (correlates with the nature of defects) were also determined. Using the lifetime of the third component, the radii of the nanopores (R_3) were determined according to the Tao–Eldrup model.[52]

Acknowledgements

H.K. and Y.K. would like to thank the Ministry of Education and Science of Ukraine (project for young researchers No. 0122U000807) as well as Dr. A. Ingram for assistance in PAL experiments. I.K. and H.K. would like to thank the National Research Foundation of Ukraine, project 2020.02/0217. In addition, the research on AIP has been supported by the Latvian-Ukrainian Grant LV-UA/2021/5. The Institute of Solid State Physics, University of Latvia (Latvia) as the Centre of Excellence has received funding from the European Union's Horizon 2020 Framework.

Conflict of Interest

The authors declare no conflict of interest.

Data Availability Statement

The data that support the findings of this study are available from the corresponding author upon reasonable request.

Keywords

agglomeration, ceramics, fragmentation, free-volume defects, positron annihilation

Received: September 17, 2021
Revised: May 17, 2022
Published online: June 15, 2022

[1] L. L. Noto, D. Poelman, V. R. Orante-Barrón, H. C. Swart, L. E. Mathevula, R. Nyenge, M. Chithambo, B. M. Mothudi, M. S. Dhlamini, *Physica B* **2018**, *535*, 268.
[2] M. Kodu, T. Avarmaa, H. Mändar, R. Jaaniso, *Appl. Phys. A* **2008**, *93*, 801.
[3] D. Gust, T. A. Moore, A. L. Moore, *Acc. Chem. Res.* **2009**, *42*, 1890.
[4] N. Skillen, P. K. Robertson, in *Solar Energy* (Ed: G. M. Crawley), World Scientific, Singapore **2016**, chapter 6, pp. 205–241.
[5] W. Acuna, J. F. Tellez, M. A. Macias, P. Roussel, S. Ricote, G. H. Gauthier, *Solid State Sci.* **2017**, *71*, 61.
[6] T. Guérineau, C. Strutynski, T. Skopak, S. Morency, A. Hanafi, F. Calzavara, Y. Ledemi, S. Danto, T. Cardinal, Y. Messaddeq, E. Fargin, *Opt. Mater. Express* **2019**, *9*, 2437.
[7] J. M. Gonçalves, R. A. Munoz, L. Angnes, *J. Mater. Chem.* **2021**, *100*, 8842.
[8] D. Nakauchi, G. Okada, N. Kawaguchi, T. Yanagida, *Opt. Mater.* **2019**, *87*, 58.
[9] T. A. Khattab, M. Abd El-Aziz, M. S. Abdelrahman, M. El-Zawahry, S. Kamel, *Luminescence* **2020**, *35*, 478.
[10] L. Yu, D. Den Engelsen, K. Gorobez, G. R. Fern, T. G. Ireland, C. Frampton, J. Silver, *Opt. Mater. Express* **2019**, *9*, 2175.
[11] V. M. Maphiri, M. R. Mhlongo, T. T. Hlatshwayo, T. E. Motaung, L. F. Koao, S. V. Motloung, *Opt. Mater.* **2020**, *109*, 110244.
[12] D. den Engelsen, G. R. Fern, T. G. Ireland, F. Yang, J. Silver, *Opt. Mater. Express* **2020**, *10*, 1962.
[13] D. den Engelsen, G. R. Fern, T. G. Ireland, J. Silver, *ECS J. Solid State Sci. Technol.* **2020**, *9*, 026001.
[14] N. J. Shivaramu, E. Coetsee, W. D. Roos, K. R. Nagabhushana, H. C. Swart, *J. Phys. D: Appl. Phys.* **2020**, *53*, 475305.
[15] Q. Xie, B. Li, X. He, M. Zhang, Y. Chen, Q. Zeng, *Materials* **2017**, *10*, 1198.
[16] S. Wang, Y. Wang, H. Gao, J. Li, L. Fang, X. Yu, S. Tang, X. Zhao, G. Sun, *Optik* **2020**, *221*, 165363.
[17] M. Malkamäki, A. J. Bos, P. Dorenbos, M. Lastusaari, L. C. Rodrigues, H. C. Swart, J. Hölsä, *Physica B* **2020**, *593*, 411947.
[18] D. Nakauchi, G. Okada, T. Kato, N. Kawaguchi, T. Yanagida, *Radiat. Meas.* **2020**, *135*, 106365.
[19] M. Vrankić, A. Šarić, S. Bosnar, D. Pajić, J. Dragović, A. Altomare, A. Falcicchio, J. Popović, M. Jurić, M. Petravić, I. Jelovica Badovinac, G. Dražić, *Sci. Rep.* **2019**, *9*,, 15158.
[20] M. G. Brik, A. Suchocki, A. Kaminska, *Inorg. Chem.* **2014**, *53*, 5088.
[21] Y. Wang, W. B. Chen, F. Y. Liu, D. W. Yang, Y. Tian, C. G. Ma, M. D. Dramićanin, M. G. Brik, *Results Phys.* **2019**, *13*, 102180.
[22] A. Luchechko, Y. Zhydachevskyy, S. Ubizskii, O. Kravets, A. I. Popov, U. Rogulis, E. Elsts, E. Bulur, A. Suchocki, *Sci. Rep.* **2019**, *9*, 9544.
[23] M. G. Brik, N. M. Avram, C. N. Avram, C. Rudowicz, Y. Y. Yeung, P. Gnutek, *J. Alloys Compd.* **2007**, *432*, 61.
[24] I. Karbovnyk, J. Collins, I. Bolesta, A. Stelmashchuk, A. Kolkevych, S. Velupillai, S. H. Klym, O. Fedyshyn, S. Tymoshuk, I. Kolych, *Nanoscale Res. Lett.* **2015**, *10*, 151.
[25] S. V. Lisovskii, A. V. Meganov, V. R. Khrustov, V. V. Ivanov, *J. Phys. Conf. Ser.* **2019**, *1410*, 012089.
[26] D. Valiev, O. Khasanov, E. Dvilis, S. Stepanov, V. Paygin, A. Ilela, *Phys. Status Solidi B* **2020**, *257*, 1900471.
[27] Q. Chen, L. Shang, H. Xu, C. Ma, C. K. Duan, *J. Phys. Chem. C* **2021**, *125*, 21780.
[28] A. Lushchik, E. Feldbach, E. A. Kotomin, I. Kudryavtseva, V. N. Kuzovkov, A. I. Popov, V. Seeman, E. Shablonin, *Sci. Rep.* **2020**, *10*, 7810.
[29] N. Mironova-Ulmane, A. I. Popov, G. Krieke, A. Antuzevics, V. Skvortsova, E. Elsts, A. Sarakovskis, *Low Temp. Phys.* **2020**, *46*, 1154.
[30] A. Platonenko, D. Gryaznov, E. A. Kotomin, A. Lushchik, V. Seeman, A. I. Popov, *Nucl. Instrum. Methods Phys. Res., Sect. B* **2020**, *464*, 60.
[31] Q. Li, T. Liu, X. Xu, X. Wang, R. Guo, X. Jiao, Y. Lu, *Mater. Technol.* **2021**, *36*, 279.
[32] Q. Li, T. Liu, X. Xu, R. Guo, X. Jiao, X. Wang, Y. Lu, *J. Phys. Chem. Solids* **2020**, *145*, 109542.
[33] V. Seeman, E. Feldbach, T. Kärner, A. Maaroos, N. Mironova-Ulmane, A. I. Popov, E. Shablonin, E. Vasil'chenko, A. Lushchik, *Opt. Mater.* **2019**, *91*, 42.
[34] O. V. Ogorodnikova, M. Majerle, J. Čížek, S. Simakov, V. V. Gann, P. Hruška, J. Kameník, J. Pospíšil, M. Štefánik, M. Vinš, *Sci. Rep.* **2020**, *10*, 18898.
[35] R. Rementeria, R. Domínguez-Reyes, C. Capdevila, C. Garcia-Mateo, F. G. Caballero, *Sci. Rep.* **2020**, *10*, 486.
[36] D. V. Barad, P. L. Mange, K. K. Jani, S. Mukherjee, M. Ahmed, S. Kumar, S. N. Dolia, R. Pandit, P. Y. Raval, K. B. Modi, P. M. G. Nambissan, *Ceram. Int.* **2021**, *47*, 2631.
[37] H. Klym, A. Ingram, I. Hadzaman, I. Karbovnyk, I. Vasylchyshyn, A. I. Popov, *IOP Conf. Ser.: Mater. Sci. Eng.* **2019**, *503*, 012019.
[38] A. H. Ghanem, K. R. Mohamed, *Arab J. Nucl. Sci. Appl.* **2021**, *54*, 98.
[39] H. I. Zhang, S. Sellaiyan, K. Sako, A. Uedono, Y. Taniguchi, K. Hayashi, *Polymer* **2020**, *190*, 122225.
[40] D. Biswas, A. Rajan, S. Kabi, A. S. Das, L. S. Singh, P. M. G. Nambissan, *Mater. Charact.* **2019**, *158*, 109928.
[41] O. Melikhova, J. Kuriplach, I. Prochazka, J. Cizek, M. Hou, E. Zhurkin, S. Pisov, *Appl. Surf. Sci.* **2008**, *255*, 157.
[42] J. Filipecki, A. Ingram, H. Klym, O. Shpotyuk, M. Vakiv, *J. Phys. Conf. Ser.* **2007**, *79*, 012015.
[43] H. Klym, I. Hadzaman, V. Gryga, *Appl. Nanosci.* **2021**, *12*, 1257.
[44] O. Shpotyuk, V. Balitska, M. Brunner, I. Hadzaman, H. Klym, *Physica B* **2015**, *459*, 116.
[45] H. Klym, A. Ingram, O. Shpotyuk, I. Karbovnyk, *Opt. Mater.* **2016**, *59*, 39.
[46] H. Klym, A. Ingram, O. Shpotyuk, *Materialwiss. Werkstofftech.* **2016**, *47*, 198.
[47] H. Klym, A. Ingram, *J. Phys. Conf. Ser.* **2007**, *79*, 012014.
[48] Y. Kostiv, A. Luchechko, H. Klym, I. Karbovnyk, B. Sadovyi, O. Zaremba, O. Kravets, in *XIth Inter. Scientific and Practical Conf. on Electronics and Information Technologies*, IEEE, Lviv, Ukraine **2019**, p. 307.
[49] A. Luchechko, O. Kravets, *Phys. Status Solidi C* **2017**, *14*, 1600146.
[50] J. Kansy, D. Giebel, *J. Phys. Conf. Ser.* **2011**, *265*, 012030.
[51] A. Bondarchuk, O. Shpotyuk, A. Glot, H. Klym, *Rev. Mex. Fis.* **2012**, *58*, 313.
[52] T. Goworek, *Chem. Phys. Lett.* **2002**, *366*, 184.

